

Experimental study on carbon nanofluid pressure drop and pumping power

Received 30th August 2019,
Accepted 11th December 2019,
DOI:10.22126/anc.2019.4418.1015

Amir Hossein Shiravi¹, Mohammad Firoozzadeh^{*1}, Hadis Bostani¹, Mojtaba Shafiee²,
Maryam Bozorgmehrian¹

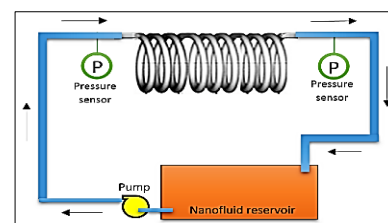
¹Department of Mechanical Engineering, Jundi-Shapur University of Technology, Dezful, Iran

²Department of Chemical Engineering, Jundi-Shapur University of Technology, Dezful, Iran

Abstract

The nanofluids have been able to occupy an important place in engineering, in spite of being a young science. While nanoparticles are very effective in increasing heat transfer of base fluids, they cause a significant pressure drop in the flow. In this paper, the effect of different concentrations, 0.1 to 0.4 wt.%, of carbon nanofluid in water have been investigated on the pressure drop of fluid flow over the Reynolds range from 14,000 to 28,000. The variation of pumping power was measured and the corresponding results illustrated increasing in the friction factor of the nanofluid at concentration 0.4 up to 70%, leading to a 68% increase in the pumping power.

Keywords: Nanofluid, Friction factor, Pressure drop, Pumping power.



Introduction

Nanoscience has become one of the effective parts of various fields such as sensors,¹ medical science,^{2,3} wastewater,⁴ energy,^{5,6} nano-chemistry,⁷ and so on. Adding nanoparticles leads to an increase in a convective heat-transfer rate of a fluid, however, it has a negative effect on the pressure drop, which has been investigated by some researchers. For example, Lee and Mudawar⁸ discussed the effect of aluminum oxide/water nanofluid on pressure drop in a mini-channel. They showed that the pressure drop of nanofluid was higher than that of based fluid and increased with the increase of nanoparticle concentration at the same Reynolds number.

Vajja et al.⁹ experimentally studied Al₂O₃/water in a pipe, for Reynolds of 6700 and displayed the more pressure drop *ca.* a 10% compared with pure water. Sundar et al.¹⁰ have investigated the friction factor of Fe₂O₃/water as nanofluid with the volume concentration of 0.6 vol.% in the turbulent flow. They achieved 10% increase in the friction factor compared with pure water.

Pourfarhang et al.¹¹ studied the CuO/water-ethylene glycol nanofluid in various inlet fluid temperatures, where, the based fluid was made of 60% ethylene glycol and 40% water. In this study, it was revealed that increasing the inlet temperature in a constant Reynolds (*Re*) number increased the friction factor. In a different study, Lalegani et al.¹² investigated the effect of various wall roughness on friction factor in laminar flow. They illustrated that the values of both pressure drop and friction factor, are increased by growing the size of the roughness elements.

Using insert is known as a popular and industrial method for increasing heat transfer in heat exchangers. Gorjæi and Shahidian¹³ compared the friction factor of a tube, in the cases of with and

without the twisted tape insert. They selected the turbulent regime for their tests. Finally, it was found that using twisted tape insert, leads to an increase of about 31% and 35% in heat transfer and friction factor, respectively. A CuO/oil nanofluid was investigated by Saeedinia et al.¹⁴ and illustrated a 63% jump in pressure drop when the mentioned nanofluid flows through a pipe with coiled insert in a laminar flow. In other research, Fotukian and Esfahany¹⁵ studied the pressure drop in CuO/water nanofluid in turbulent flow, using a circular pipe. They showed that the addition of the mentioned nanoparticles to water leads to a 20% increase in the pressure drop, compared with pure water. In another work, Hussein et al.¹⁶ investigated the effect of adding 0.017 vol.% graphene to Al₂O₃/water nanofluid and observed a 15% increase in pressure drop. Esfe et al.¹⁷ have also studied the pressure drop of multi-walled carbon nanotube (MWCNT)/water nanofluid and reported an increase of 27.3% in pressure drop in the concentration of 1 vol.%, compared with pure water. Hosseinipour et al.¹⁸ studied the effect of adding different mass concentrations of MWCNT to water in laminar regime, under a constant heat flux. They showed that low concentrations of MWCNT had a minor effect on the improvement of pressure drop. Both convective heat transfer and friction factor of silver nanofluid in various concentrations of 1-5 vol.% were also investigated by Waghole et al.¹⁹ They used a straight pipe equipped with various twisted tape inserts and tests were carried out in Reynolds range of 500 to 6,000. Consequently, they revealed a new correlation for predicting both heat transfer and friction factor for the conditions of their experiments.

As already mentioned, by increasing in nanofluid concentration, the friction factor is increased. Hence, some scholars tried to diminution this problem. Paryani and Ramazani²⁰ have an experimental study on Nusselt and pressure drop of TiO₂/water

Corresponding author:

Mohammad Firoozzadeh, Email: firooz_mechanic@yahoo.com

nanofluid at Reynolds number between 11,000 and 12,000. They showed that TiO₂ has the best thermal performance at 0.02 vol.% concentration. Moreover, in order to reduce the effect of nanoparticles on friction factor, they added polyacrylamide in nanofluid, which had no significant effect on heat transfer, while by decreasing the drag force of nanofluid, the friction factor was decreased. It was found from their experiments that adding only 55 ppm of polyacrylamide to water could decrease the friction factor by about 33%. More information and correlation about convective heat transfer and friction factor in tubes can be found in.²¹⁻²⁴

In this paper, we investigated the effect of adding carbon nanoparticles to water and measured its effect on friction factor. Moreover, the experimental results have been compared with the analytical one, in order to find the best formula for estimating the pressure drop behavior of carbon/water nanofluid. In addition, the influence of pressure difference due to adding nanoparticles on pumping power has been calculated.

Experimental

Preparation of nanofluid

In this study, we used carbon black nanoparticles. The source of carbon nanoparticles is Sadaf Doodeh Fam Co. The data of carbon nanoparticles in Table 1 have been obtained from the report of this company.

Various weight concentrations of carbon nanoparticles in water, include 0.1, 0.2, 0.3, and 0.4 wt.%, have been tested. Moreover, in order to minimize the sedimentation rate, sodium dodecyl sulfate (SDS) was used as a surfactant. All of the required properties of carbon, SDS, and water are presented in Table 1. The transmission electron microscopy (TEM) image of carbon nanoparticles is depicted in Figure 1 that indicates their mean diameter of particles about 100 nm. In order to have better stability in the nanofluid, carbon nanoparticles and SDS were mixed by a 1:1 ratio in water. This process was made using a mixer followed by an ultrasonic device. It was found that SDS significantly increased the stability of carbon in water, so that, an acceptable mixture stability was kept, even after 7 days (Figure 2).

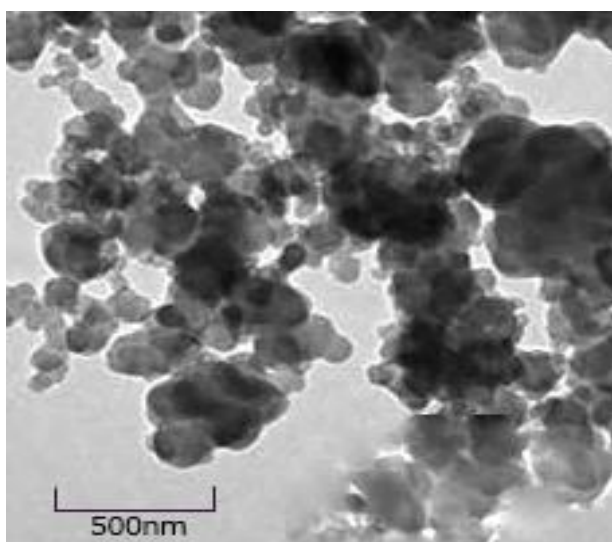


Figure 1. The TEM image of carbon nanoparticles.

Table 1. Chemical characteristics of carbon nanoparticles and SDS.

Material	Specific heat capacity (J kg ⁻¹ K ⁻¹)	Density (kg m ⁻³)	Thermal conductivity (W mK ⁻¹)	Kinematic viscosity (m ² s ⁻¹)	Reference
Carbon	709	2050	168	-	-
Water	4179	997	0.613	1.0 E ⁻⁶	25
SDS	N/A	1010	0.58	-	26



Figure 2. Stability of nanofluid after 7 days for (a) without SDS and (b) with SDS.

Experiment procedure

To measure the pressure drop value of nanofluids in a helically-coiled tube, a device was built at Jundi-Shapur University of technology, Dezful, Iran (Figure 3). In this device, two pressure sensors, made by Hogler Company, with the accuracy of 0.5% were installed on the inlet and outlet of the helically-coiled tube. These sensors can measure the pressure in the range of 0 to 4 bar.



Figure 3. An image of the experimental set-up.

A Schematic view of the experimental set-up and the specifications of helical coiled have been illustrated in Figure 4 and Table 2, respectively. The carbon nanofluid is circulated in the system with various flow rates. The utilized pump can provide the Reynolds range of 3,000 to 30,000. The Reynolds range of 14,000 to 28,000 is considered in the experiments. In this range, 15 different flow rate intervals were selected and the pressure drop was measured for different concentrations of carbon nanofluid. The uncertainty of the experimental setup was investigated according to the proposed method in reference.²⁷ The uncertainty of calculated pumping power and friction factor was calculated to be 3.3% and 4.3%, respectively.

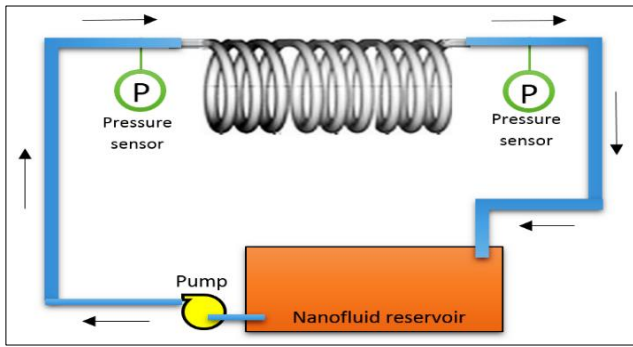


Figure 4. A schematic view of the experimental set-up.

Table 2. The specifications of the helical coil.

Parameters	Dimensions
Tube length	6 m
Tube diameter	3/8 inch
Coil length	20 cm
Coil diameter	10 cm
Material	Copper

Governing equations

The Darcy–Weisbach equation, is a common equation to calculate the friction factor, as follows:²⁰

$$f = \frac{\Delta P}{\left(\frac{L}{D_i}\right)\left(\frac{\rho u^2}{2}\right)} \quad (1)$$

where ΔP is the pressure drop from inlet to outlet in (Pa), L and D_i are geometric parameters of the coiled tube, which are the length and inner diameter of the tube in (m), respectively. The density of the fluid is shown by ρ in (kg m^{-3}) and u is the average velocity of the fluid in (m s^{-1}).

As described previously, in this research, a helically-coiled tube was considered. So, another equation for the specific use of this type of heat exchanger is the equation presented by Mori and Nakayama²⁸ in 1967, equation (2):²⁸

$$f = \frac{64}{Re} (Re \delta_r^2)^{\frac{1}{20}} \quad (2)$$

where δ_r is the ratio of the coil-to-tube radii. More equations for friction factor calculation have been listed in Table 3.

In addition to the friction factor, the pumping power was also investigated. More pumping power means more electricity requirement. So, pumping power is considered as an important parameter in both economic and technical assessments.

Table 3. Different correlations for calculating the friction factor.

Correlation	Remark	Reference
$f = [1.58 \ln Re - 3.82]^{-2}$	$2300 < Re < 5 \times 10^6$, $0.5 < Pr < 2000$	29
$f = [0.79 \ln Re - 1.64]^{-2}$	$3000 < Re < 5 \times 10^6$	30
$f = \frac{64}{Re} (Re \cdot \delta_r)^{1/20}$	Used for coiled tube heat exchangers, in turbulent regime	28
$f = 0.37 \left(\frac{64}{Re}\right) (Re \cdot \delta_r)^{0.36}$	Used for coiled tube heat exchangers, in laminar regime	31
$f = 0.3164 Re^{-0.25}$	$3000 < Re < 5 \times 10^6$	32,33

Pumping power can be defined in relation to either heat transfer³⁴ or pressure drop.²⁵ Since we focused on the effect of nanoparticles on pressure drop of the fluid, the relationship between pumping power and pressure variation is considered as follows:²⁵

$$\text{Pumping Power} = \left(\frac{\dot{m}}{\rho_{nf}}\right) \Delta P \quad (3)$$

where, \dot{m} is the mass flow rate of nanofluid, which is calculated as follows:

$$\dot{m} = \frac{\pi}{4} Re d \mu_{nf} \quad (4)$$

In equations (3) and (4), ρ_{nf} and μ_{nf} are density and dynamic viscosity of nanofluid, respectively. These parameters are calculated as follows:^{35,36}

$$\rho_{nf} = \rho_p \varphi + (1 - \varphi) \rho_{nf} \quad (5)$$

and;

$$\mu_{nf} = \frac{\mu_f}{(1 - \varphi)^{2.5}} \quad (6)$$

Where, φ is the nanofluid concentration.

Results and discussion

In this paper, by measuring the pressure drop in the helically-coiled tube in various concentrations of carbon nanofluid, both friction factor and pumping power are calculated. Afterwards some comparisons between our results and other researches have been carried out.

Friction factor

The influence of different concentrations of carbon nanofluid on friction factor has been presented in Figure 5. It is obvious that the based fluid has the lowest friction factor and increasing the nanofluid concentration leads to a significant increase in the friction factor, compared to the based fluid. The mean increase of 5, 18.4, 40.1, and 70.2% have been observed for concentrations 0.1, 0.2, 0.3, and 0.4 wt.%, respectively. In the other hand, the lowest concentration of carbon nanofluid caused the lowest difference in the friction factor when compared with pure water, which is in complete agreement with Kahani et al. report.³⁷

Variations in the value of Reynolds number are another effective parameter that strongly influences the pressure drop and friction factor. As observed in Figure 5, Reynolds number and friction factor are inversely related. So, increasing in Reynolds number leads to a decrease in friction factor. According to equation (2), δ_r plays a geometrical role for friction factor of a helical coiled. Therefore, increasing in δ_r leads to a tiny increase in friction factor.

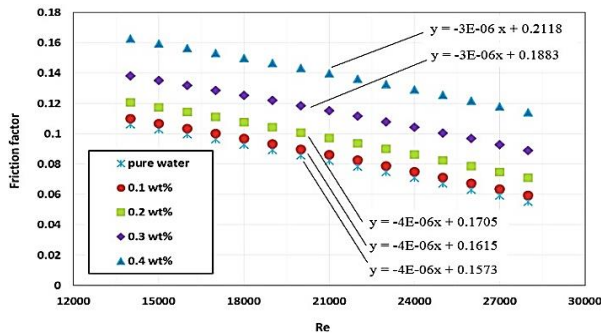


Figure 5. Friction factor versus Re , in different concentrations of carbon nanofluid.

The results of the comparison of the experimental results with the analytical one are shown in Figure 6. The experimental results of pure water are compared with four different formulas, which are presented in Table 3. It is observed that our results have an acceptable agreement with Mori and Nakayama formula, which is for the specific use of the helically-coiled tube. The wane trend of increasing turbulence on friction factor has been also illustrated in this figure.

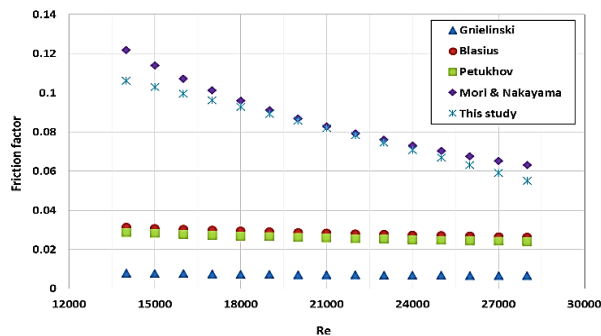


Figure 6. Comparison of experimental and analytical results for friction factor.

Pumping power

As already mentioned, the optimization of pumping power plays an important role in the energy saving of the system.³⁸ So, the variation of pumping power versus Reynolds number has been depicted in Figure 7. Obviously, increasing in Reynolds number leads to an increase in pumping power. Moreover, in higher Reynolds numbers, this influence is more remarkable. Nanofluid concentration is another factor which leads to augment the pumping power. As shown in Figure 7, higher concentrations require higher pumping power. Given the linear behavior for the curves in Figure 7, the mentioned relationships on the figure are reportable.

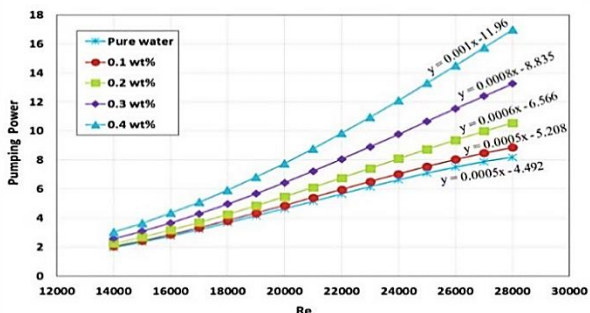


Figure 7. Effect of nanofluid concentration and Reynolds (Re) number on pumping power.

To have a better conclusion, it can be reported that in Reynolds number of 21,000, which is the average of Reynolds values of our investigations, the pumping power addition of 4.8, 16.9, 38.5, and 68.3% were revealed for concentrations of 1, 2, 3, and 4 wt.%, respectively. Therefore, at 0.1 wt.% that is the lowest concentration of carbon nanoparticles, the pumping power is not notably different from the based fluid. Moreover, according to Figure 7, increasing Reynolds number leads to the increase of pumping power. So that in lower Reynolds number, the difference between pumping power of various concentrations is tiny and by increasing in the Reynolds number the mentioned difference is increased.

Conclusion

In this paper, the pressure drop caused by adding nanoparticles to water is investigated experimentally, through a helically-coiled tube. Experiments were carried out in various Re numbers, and the influence of Re on pressure drop was investigated, too. The experimental results were compared with the analytical formulae and good agreement was observed with Mori and Nakayama equation. Besides, it was shown that adding nanoparticles considerably affects the pressure drop in the helical tube, and the higher the concentrations, the greater the effect on pressure drop. So, at a mass concentration of 0.4%, more than 70% increase in pressure drop has occurred. Finally, the increase in pumping power as an important engineering parameter was calculated and it was revealed that in the concentration of 0.4 wt.% of carbon nanofluid and Reynolds number of 21000, there was a 68% increase in pumping power.

References

1. J. Ghodsi, A.A. Rafati, and Y. Shoja, *Adv. Nanochem.*, **1**, **2019**, 6.
2. F. Mousavi and A.A. Taherpour, *Adv. Nanochem.*, **1**, **2019**, 12.
3. K. Sayyadi, A. Rahdar, N. Esmaili, and J. Sayyadi, *Adv. Nanochem.*, **1**, **2019**, 47.
4. N. Noori and N. Fattahi, *Adv. Nanochem.*, **1**, **2019**, 17.
5. M. Firoozzadeh, A.H. Shiravi, and M. Shafiee, *J. Solar Energy Res.*, **3**, **2018**, 287.
6. M. Firoozzadeh, A.H. Shiravi, and M. Shafiee, *Iran. J. Energy Environ.*, **10**, **2019**, 80.
7. N. Faizbakhsh and Z. Safari, *Adv. Nanochem.*, **1**, **2019**, 52.
8. J. Lee and I. Mudawar, *Int. J. Heat Mass Transf.*, **50**, **2007**, 452.
9. R.S. Vajjha, D.K. Das, and D.P. Kulkarni, *Int. J. Heat Mass Transf.*, **53**, **2010**, 4607.
10. L.S. Sundar, M. Naik, K. Sharma, M. Singh, and T.C.S. Reddy, *Exp. Therm. Fluid Sci.*, **37**, **2012**, 65.
11. P. Samira, Z.H. Saeed, S. Motahare, and K. Mostafa, *Korean J. Chem. Eng.*, **32**, **2015**, 609.
12. F. Lalegani, M.R. Saffarian, A. Moradi, and E. Tavousi, *Int. J. Numer. Method H.*, **28**, **2018**, 1664.
13. A. Rezaei Gorjaei and A. Shahidian, *J. Therm. Anal. Calorim.*, **137**, **2019**, 1059.
14. M. Saeedinia, M. Akhavan-Behabadi, and M. Nasr, *Exp. Therm. Fluid Sci.*, **36**, **2012**, 158.
15. S. Fotukian and M.N. Eshfahny, *Int. Commun. Heat Mass*, **37**, **2010**, 214.
16. A.A. Hussien, N.M. Yusop, M.d.A. Al-Nimr, M.Z. Abdullah, A.A. Janvekar, and M.H. Elnaggar, *Iran J. Sci. Technol. A.*, **43**, **2019**, 1989.
17. M.H. Esfe, S. Saedodin, O. Mahian, and S. Wongwises, *Int. Commun. Heat Mass*, **58**, **2014**, 176.
18. E. Hosseinipour, S.Z. Heris, and M. Shanbedi, *J. Therm. Anal. Calorim.*, **124**, **2016**, 205.

19. D.R. Waghole, R.M. Warkhedkar, V.S. Kulkarni, and R.K. Shrivastva, *Heat Mass Transfer*, 52, **2016**, 309.
20. S. Paryani and A. Ramazani SA, *Can. J. Chem. Eng.*, 96, **2018**, 1430.
21. L.S. Sundar and M.K. Singh, *Renew. Sust. Energ. Rev.*, 20, **2013**, 23.
22. M. Kahani, S. Zeinali Heris, and S.M. Mousavi, *Ind. Eng. Chem. Res.*, 52, **2013**, 13183.
23. S. Hosseini, M. Sheikholeslami, M. Ghasemian, and D. Ganji, *Powder Technol.*, 324, **2018**, 36.
24. M. Firoozzadeh, A.H. Shiravi, and M. Shafiee, *Iran. J. Energy Environ.*, 10, **2019**, 23.
25. A. Falahat, M. Shabani, and M. Maleki, *J. Mech. Eng. Tech.*, 7, **2015**.
26. R. Saeed, M. Usman, A. Mansha, N. Rasool, S.A.R. Naqvi, A.F. Zahoor, H.M.A. Rahman, U.A. Rana, and E. Al-Zahrani, *Colloid Surface A*, 512, **2017**, 51.
27. R. Moradi, M.R. Saffarian, and M. Behbahani-Nejad, *J. Therm. Anal. Calorim.*, **2019**, (Available Online).
28. Y. Mori and W. Nakayama, *Int. J. Heat Mass Transf.*, 10, **1967**, 681.
29. V. Gnielinski, *Int. Chem. Eng.*, 16, **1976**, 359.
30. B.S. Petukhov, *Advances in Heat Transfer*, eds. J.P. Hartnett, T.F. Irvine, Elsevier, (1970), vol. 6.
31. H. Itō, *J. Basic Eng.*, 81, **1959**, 123.
32. H. Blasius, *Mitteilungen über Forschungsarbeiten auf dem Gebiete des Ingenieurwesens*, Springer, (1913), Berlin, Germany, ch. 1.
33. P. Mishra and S. Gupta, *Ind. Eng. Chem. Process Des. Dev.*, 18, **1979**, 130.
34. A. Vosough and A. Falahat, *J. Thermophys. Heat Tr.*, 26, **2012**, 141.
35. B.C. Pak and Y.I. Cho, *Exp. Heat Transfer*, 11, **1998**, 151.
36. H. Brinkman, *J. Chem. Phys.*, 20, **1952**, 571.
37. M. Kahani, S.Z. Heris, and S.M. Mousavi, *Heat Mass Transf.*, 50, **2014**, 1563.
38. M. Shanbedi, A. Amiri, S.Z. Heris, H. Eshghi, and H. Yarmand, *J. Therm. Anal. Calorim.*, 131, **2018**, 1089.